5 Silicosis

Clara Gaik Cheng Ooi and Hiroaki Arakawa

CONTENTS

5.1 Introduction

Silicosis is an occupational lung disease caused by inhalation of silica, a ubiquitous mineral found in abundance in the earth's crust, composed of regular molecules of silicon dioxide (SiO_2). Certain occupations predispose the individual to high concentrations of silica, which is fibrogenic to the lungs, resulting in radiographic and pathological abnormalities. Workers engaged in occupations such as tunneling, mining, sandblasting and quarrying are inevitably exposed to the mineral, due to its ubiquity in the earth's crust. Other occupations, such as work with gemstones, including jade polishers (White et al. 1991; Gupta et al. 1991; Ng et al. 1985), foundry and pottery workers (Landrigan et al. 1986; Rees et al. 1992; Epstein et al. 1984) and glass and silica bricks workers (Landrigan et al. 1986), are associated with silica exposure. The diagnosis of silicosis is based on the typical radiographic appearance of diffuse nodules or reticulonodular pattern in the presence of a strong occupational exposure to silica. The International Labour Organization (ILO) 2000 International Classification of Radiographs of the Pneumoconiosis is the most commonly accepted classification of extent of involvement of the pneumoconiosis and one in which the presence or absence of pneumoconiosis is established in workers exposed to mineral dust including silica (Geneva, International Labour Office 2000; Davies 1974). Standard reference radiographs are available from the ILO office with standard nomenclature to describe the changes.

5.2 Pathogenesis

The role of macrophages in the pathogenesis of silicosis has been extensively studied (Davis and Gemsa 1996; Harmsen et al. 1985; Corry et al. 1984; Lehnert et al. 1986; Graham 1992). Inhaled crystalline silica smaller than 5 μm are deposited in the small airways and alveoli from which they are ingested within 48 h of deposition by alveolar macrophages or tissue macrophages, if they penetrate the interstitium. Free particulate silica that are not ingested by macrophages enter the perivascular lymphatic channels to be translocated to the draining mediastinal lymph nodes as free particles or within macrophages (Davis and Gemsa 1996; Harmsen et al. 1985; Corry et al. 1984; Absher et al. 1992; Lauweryns and Baert 1977). In vivo and in vitro studies have shown that these silica-exposed macrophages release fibroblast growth fac-

C. G. C. Ooi, MD
Department of Diagnostic Radiology, University of Hong Kong, Queen Mary Hospital, Pokfulam Road, Pokfulam, Hong Kong SAR, China
H. Arakawa, MD
Department of Radiology, Dokkyo University School of Medicine, 880, Mibu, Tochigi, 321-0293 Japan

tors that facilitate the accumulation of fibroblasts and fibroblast products, which induce inflammatory and fibrogenic reaction in the interstitium, alveoli and lymph nodes (Lauweryns and Baert 1977; Brown et al. 1988; Jagirdar et al. 1996; Dubois et al. 1989; Lugano et al. 1984; Hunninghake et al. 1986; Bitterman et al. 1983; Schmidt et al. 1984; Kampschmidt et al. 1986). Other inflammatory cells recruited in the lung in addition to the macrophages include lymphocytes, particularly T-helper cells and neutrophils.

5.3 Pathology

Classic (Nodular) Silicosis

Nodular silicosis is characterized by the presence of small rounded nodules of 3–6 mm in the lung parenchyma (Gibbs and Wagner 1998; Weill et al. 1994).

The nodules of silicosis are well defined and located in the perivascular and peribronchiolar interstitium as well as in the paraseptal and subpleural interstitium (Fig. 5.1) and are preferentially distributed in the upper lobes. The silicotic nodule starts as a central zone of mononuclear cells surrounded by fibroblasts and collagen tissue. With time, the central zone becomes hypocellular, with concentric laminar deposition of reticulin, proteins, phospholipids and collagen in the periphery, giving a whorled appearance (Fig. 5.1). Adjacent vessels and bronchioles may become involved and destroyed by these nodules, with occlusion of their lumen.

Conglomeration of the nodules frequently occurs to form large masses of progressive massive fibrosis (PMF), usually in the upper lobes where nodular profusion is highest. The lower lobes are less frequently involved. PMF lesions sometimes cross the interlobar fissure to form elongated masses from lung apex to the lower lobe. Although conglomeration usually occurs in heavily dust-laden lung with a high profusion of nodules, its development does not always parallel nodular profusion. Cavitation of PMF masses occurs as a result of ischemic necrosis and mycobacterial infection.

Hilar and mediastinal lymph nodes are enlarged and pigmented, with a whorled appearance similar to that found in the silicotic nodule. Calcification is also a frequent finding. Features characterized on imaging, particularly on computed tomography (CT), will reflect these pathological changes in the lungs and lymph nodes.

Mixed Dust Fibrosis

Although the radiographic characteristics of mixed dust fibrosis have not been a subject of interest in recent literature, this entity is frequently described in pathology textbooks and is of some clinical importance within the context of lung damage in silica-exposed workers (Gibbs and Wagner 1998; Weill et al. 1994). Exposure to high content (more than 18% of total dust deposited in lung) of free crystalline silica results in classic silicosis, while mixed dust fibrosis develops in the presence of low silica content (less than 18% of total dust deposited in lung) (Nagelschmidt 1960), particularly with simultaneous inhalation of other minerals such as non-fibrous silicate (mica, kaolin, coal, talc, fuller's earth, etc.). These non-fibrous silicates augment the strong fibrotic effect of crystalline silica (Gibbs and Wagner 1998). Instead of a well-defined, whorled appearance found in the silicotic nodule, the lesions in mixed dust fibrosis are characterized by irregular shaped fibrotic nodules (often called stellate nodules) and a predilection of the fibrotic lesion to extend into the surrounding pulmonary interstitium (Fig. 5.2). The stellate nodules are less fibrotic with less collagen and are more cellular than silicotic nodules. Calcification in the nodule is rarely observed. Depending on the proportion of crystalline silica in the inhaled dust, mixed dust fibrosis and silicotic nodules coexist in the same lung, thus forming a spectrum of pathological findings (Honma et al. 2004). The nodules of mixed dust fibrosis are also located within the center of the secondary pulmonary lobule and in the subpleural and paraseptal interstitium, with upper lobe predominance.

Silicoproteinosis

The principal finding in silicoproteinosis is the presence of surfactant protein filling the alveolar spaces, as is seen in acquired form of alveolar proteinosis (Gibbs and Wagner 1998). Silicotic nodules are sparse and poorly demarcated or absent, probably because of a short period of time after exposure (Hoffman et al. 1973; Roeslin et al. 1980). There is diffuse alveolar wall thickening and fibrosis, as is seen in acquired form of proteinosis (Heppleston and Young 1972).

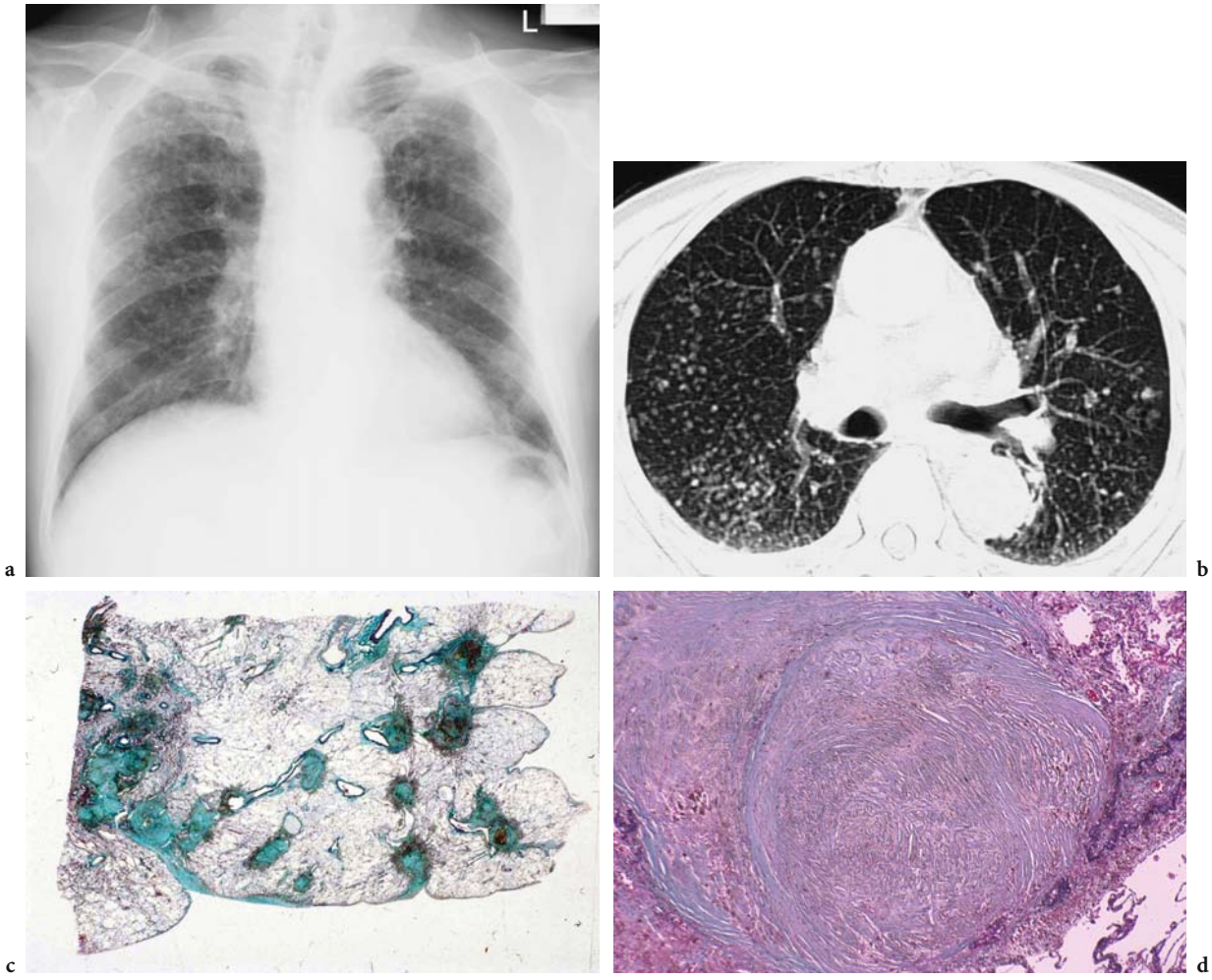

Fig. 5.1a–d. Classic silicosis in 74-year-old retired metal ore miner. **a** Posterior–anterior chest radiograph shows multiple calcified small nodules predominantly in upper lung zones. The size and profusion of the nodules are r/r and 2/2 according to the International Labour Organization classification. **b** Spiral computed tomography image (10-mm thickness) shows multiple small nodules that are most predominant in the posterior half of upper lobes. The nodules are separated with similar distance with each other, which is compatible with the centrilobular localization of silicotic nodules. **c** Photomicrograph of autopsied lung specimen (Elastic–Goldner stain) shows silicotic nodules with or without calcification along the interlobular septa and in the centrilobular areas as well as in the subpleural interstitium. The nodules are separated with equal distance with each other, suggesting a centrilobular localization. **d** Photomicrograph of a silicotic nodule shows a typical whorled appearance

5.4 Clinical Features

Unlike other inhalational occupational lung diseases, lung changes in silicosis can often progress even after the individual is removed from the dusty environment that initiated the fibrogenic lung disease (Nozaki and Sawada 1959; Lee et al. 2001). Whilst most patients are asymptomatic initially, dyspnea on exertion and then at rest is common. A relationship between severity of dyspnea and radiographic abnormalities has been documented (Ooi et al. 2003b; Koskinen 1985). With progressive lung damage, pulmonary hypertension and right heart failure eventually supervenes. Emphysema is common in silicosis and has been attributed as the major cause of cor pulmonale and disability rather than fibrosis by some investigators (Murray et al. 1993). Several studies evaluating airflow obstruction in silica-exposed workers have suggested a relationship between silica dust exposure and reduction in lung function irrespective of radiographic evidence

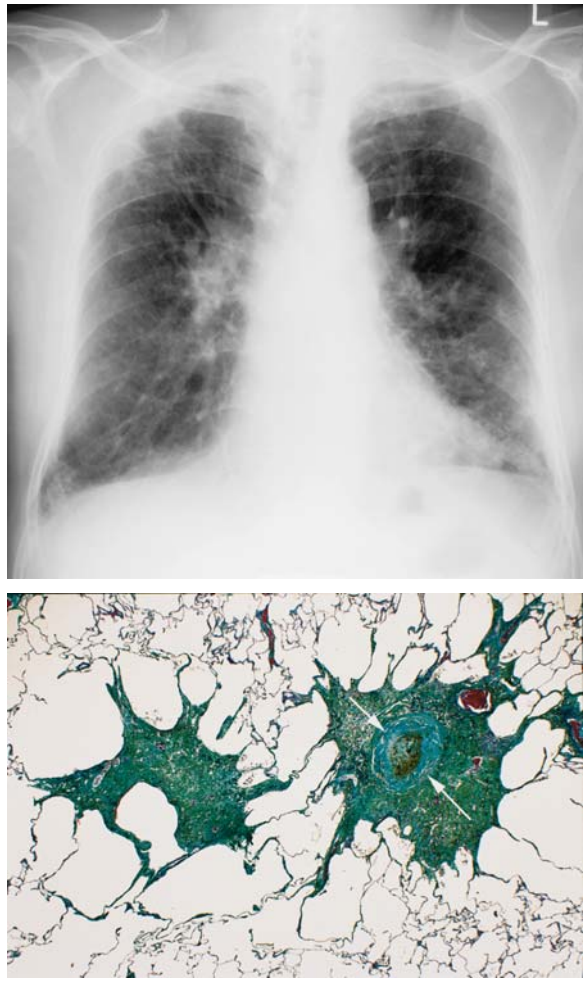

Fig. 5.2a,b. A 72-year-old retired tunnel worker with silicotic nodules and mixed dust fibrosis. **a** Posterior–anterior chest radiograph shows ill-defined multiple small nodules and reticular opacities in both upper lobes. **b** Photomicrograph obtained at autopsy performed 2 years after chest radiograph shows two pneumoconiotic nodules with stellate appearance. The left nodule shows irregular shape without whorled appearance (*arrows*) typical of silicotic nodule. The right nodule also shows irregular shape but has a central whorled appearance of silicotic nodule. Emphysema is identified around the nodules

of silicosis or fibrosis (Lee et al. 2001; Engholm and von Schamlensee 1982; Johnson et al. 1985; Neukirch et al. 1994).

The three main clinical presentations of silicosis are classic silicosis, accelerated silicosis and silicoproteinosis. Classic silicosis is the most common presentation, in which patients remain asymptomatic until after an interval of 10–20 years of continuous silica exposure, by which time radiographic evidence is present. With accelerated silicosis, the exposure time after which the disease becomes clinically evident is much shorter, ranging from 5 years to 10 years of exposure, and the rate of disease progression noticeably faster. Clinical presentation as early as 1 year after exposure and death within 5 years has been reported (Jiang et al. 2001; Elmes 1994). High concentrations of dust in a relatively confined space are thought to predispose the individual to this form of silicosis (Michel and Morris 1964; Theron et al. 1964). However, for all intents and purposes, the radiographic, clinical and pathological features of this entity are nearly indistinguishable from classic silicosis. Silicoproteinosis is another acute and progressive form of silicosis that often results in death from respiratory failure (Bailey et al. 1974). This variant of silicosis is also associated with high dust concentration in occupations such as sandblasting, tunneling and quartzite milling (Bailey et al. 1974; Oleru 1987; Hughes et al. 1982; Buechner and Ansari 1969).

5.5 Radiological Evaluation

5.5.1 Chest Radiograph

The chest radiograph remains the most convenient imaging modality by which silicosis is diagnosed and its progression monitored (Fig. 5.3). In the ILO classification of radiographs, the radiographic opacities are characterized by their size and shape. Small rounded opacities are described as “p”, “q” or “r”, according to their size (1.5 mm, 1.5–3 mm or 3–10 mm, respectively) (Fig. 5.1, Fig. 5.3, and Fig. 5.4), while irregular opacities of similar size are respectively denoted as “s”, “t” and “u”. Profusion of nodules is a measure of the concentration of small opacities per unit area or zone of lung, determined from comparison of patient’s chest radiograph with standard radiographs provided by the ILO. There are 12 categories of profusion, which represent a continuum of changes ranging from normal to severe profusion (Liddell 1963; Liddell and Lindars 1969). These can be grouped into 4 broad categories, based on the degree obscuration of vascular lung markings by the nodules: category 0 (0/0, 0/0, 0/1), when small opacities are absent or less than category 1; category 1 (1/0, 1/1, 1/2), when small opacities are present in small numbers with normal lung markings (Fig. 5.3); category 2 (2/1, 2/2, 2/3), when numerous small opacities are present and when lung markings are

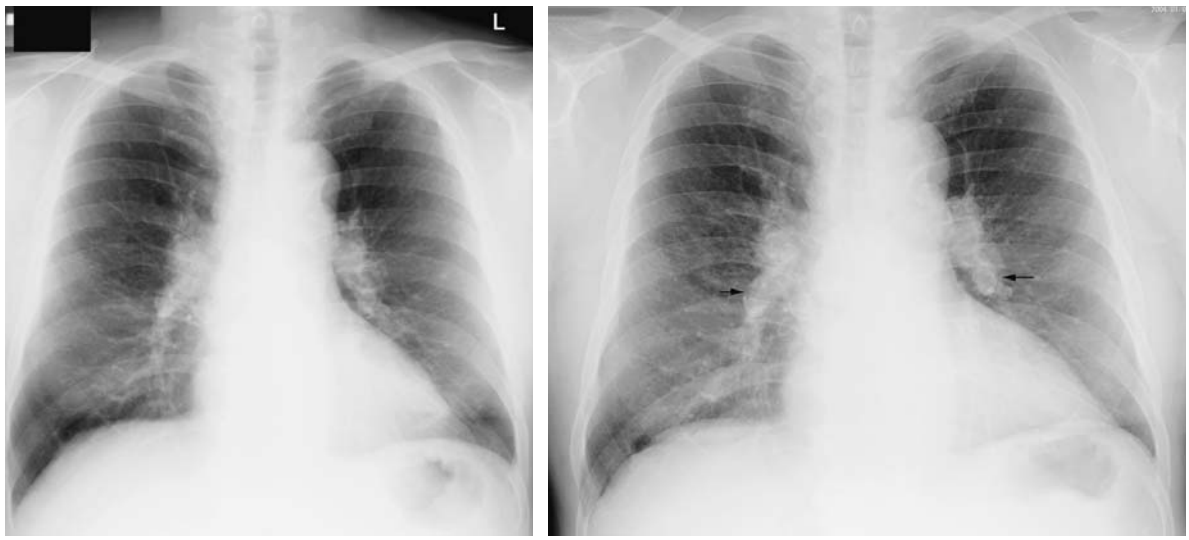

a **b**

Fig. 5.3a,b. A 67-year-old old retired tunnel worker. **a** Posterior–anterior (PA) chest radiograph obtained in 2000 showing small nodules predominantly on the upper lobe. The nodule size and profusion are p/p and 1/1 respectively. **b** PA chest radiograph obtained in 2004 show progression in the profusion of the nodules from 1/1 to 2/2. There is also more prominent egg-shell calcification of enlarged hilar lymph nodes (*arrows*)

partially obscured) (Fig. 5.1, Fig. 5.4) and category 3 (3/2, 3/3, 3/+), when very numerous small opacities totally obscure normal vascular markings (Fig. 5.4). Patients with scores 1/0 or greater are considered to have pneumoconiosis. A separate classification for large opacities (>1 cm in diameter) also exists: *A* denotes one or more opacities greater than 1 cm but each less than 50 mm; *B* indicates one or more opacities greater than A and the combined area is less than the right upper zone and *C* is used when one or more opacities has a combined area greater than the area of the right upper zone.

On the chest radiograph, the nodules in simple silicosis are well defined and small, ranging from 1 mm to 10 mm in diameter. These are present diffusely in the lungs with posterior and upper zone predominance (Bergin et al. 1986). Nodule calcification is present in up to 20% of cases on the chest

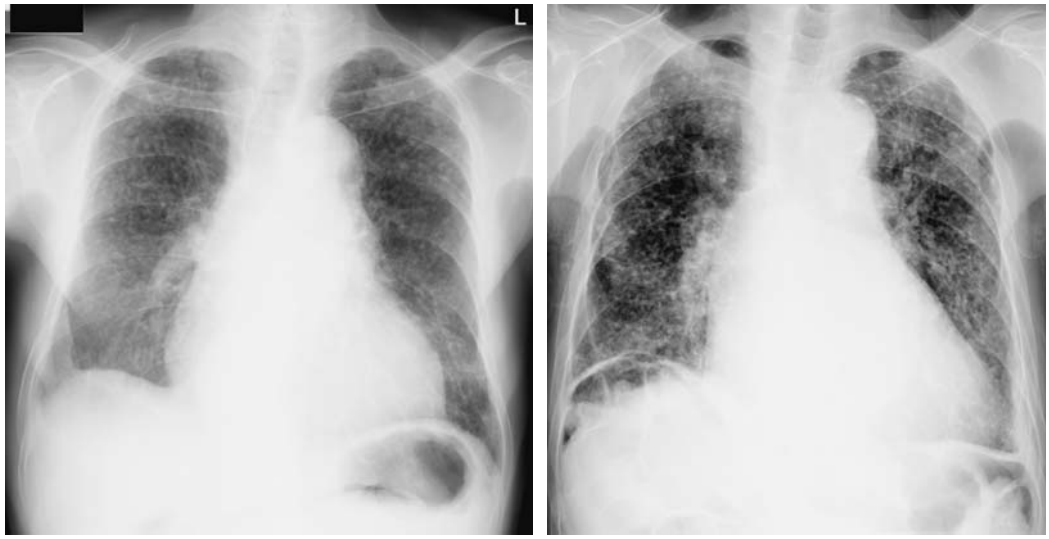

a **b**

Fig. 5.4a,b. Chest radiographs of two retired metal ore miners illustrating different categories of profusion of "r"-size nodules. **a** Posterior–anterior (PA) chest radiograph shows multiple nodules in both lungs. The nodule profusion category is 2/2. **b** PA chest radiograph shows more severe nodular profusion of category 3/3

radiograph, although the incidence is higher with CT. In "complicated silicosis" or PMF, there is conglomeration of nodules to form aggregates greater than 1 cm in diameter (Fig. 5.5). These PMF lesions are usually found in the upper zones with smooth or irregular borders. They commonly start off at the outer two-thirds of the lung, migrating centrifugally with time towards the hilum, resulting in paracicatricial emphysema between the PMF and the pleura, with volume loss in the upper lobes. With increasing severity of PMF and shrinkage of the upper lobes, reduced nodularity in the rest of the lungs will be noted (Gupta et al. 1991) (Fig. 5.5). Unilateral PMF is uncommon and, when present, can be mistaken for carcinoma of the lung.

Accelerated silicosis has similar radiographic features as the classic form of silicosis, except for its earlier onset and rapid rate of progression, which is truncated to a period of between 5 years and 10 years. Silicoproteinosis is a variant characterized by rapid and progressive involvement of the lungs with bilateral air space opacities similar to that found in alveolar proteinosis. The rate of progression ranges from a few months to a couple of years, usually culminating in death in a few years (Buechner and Ansari 1969; Dees et al. 1978).

Lymph node involvement in silicosis reflects the pathogenesis of the disease, and hilar lymphadenopathy on the chest radiograph is therefore common. "Eggshell" calcification of lymph nodes has become synonymous with silicosis, since they were first described over half a century ago and are mainly referable to the hilar lymph nodes (Fig. 5.3), although abdominal lymph nodes have also been described as bearing eggshell calcification (Jacobson et al. 1967; Jacobs et al. 1956; Gross et al. 1980). Its presence in coal and metal miners has been attributed to the concomitant exposure to silica (Jacobson et al. 1967).

Radiographic progression in silicosis is associated with the following risk factors: duration and concentration of silica exposure (Hughes et al. 1982; Saiyed and Chatterjee 1985; Ng et al. 1987; Miller et al. 1998), initial nodular profusion on chest radiograph (Lee et al. 2001; Hughes et al. 1982; Saiyed and Chatterjee 1985; Ng et al. 1987; Miller et al. 1998), simple and complicated disease (Lee et al. 2001; Saiyed and Chatterjee 1985; Ng et al. 1987; Miller et al. 1998), tuberculous infection (Jorgensen 1986), age at initial radiograph (Lee et al. 2001; Hughes et al. 1982), race (Lee et al. 2001; Hughes et al. 1982) and time interval between radiographs (Lee et al. 2001; Hughes et al. 1982). Workers who are exposed to high concentration and longer duration of dust exposure with complicated disease or tuberculous infection and who are younger at initial radiograph, are non-Caucasians and had longer duration between radiographic follow-up are reported to be more likely to have radiographic progression than their counterparts. Complicated disease on initial chest radiograph and interval of radiographic follow were independent determinants of radiographic progression in 37% of 141 granite workers with silicosis exposed to high levels of silica (Lee et al. 2001).

There are, however, limitations associated with the use of the chest radiograph in the assessment of lung changes in pneumoconiosis. This is exemplified by Epler and his colleagues, who undertook a study to determine the prevalence of normal roentgenograms in chronic diffuse infiltrative lung diseases (Epler et al. 1978). Of 458 cases of biopsy-proven chronic interstitial lung disease, 10% had a normal chest radiograph. To further illustrate the point, Kipen et al. evaluated 138 autopsy specimens with histological evidence of parenchymal fibrosis obtained from insulation workers who had died of lung cancer (Kipen et al. 1987): in 25 (18%) cases, there was no radiographic evidence of parenchymal fibrosis. Underestimation of disease, missed diagnosis and greatest inter-observer error are particularly common in subtle disease with lower categories of nodular profusion (Bégin et al. 1991; Rockoff and Schwartz 1988).

5.5.2 Computed Tomography/Thin-Section Computed Tomography

The superiority of CT, and thin-section CT over the chest radiograph in evaluating interstitial and parenchymal lung disease is well established (Epler et al. 1978; Bégin et al. 1991; Hansell and Kerr 1991; Ooi et al. 1997; Muller et al. 1989). Prior to the advent of multi-slice CT, CT evaluation of silicosis was performed using conventional or spiral CT scans comprising contiguous 7-mm or 10-mm section thickness supplemented by thin-section CT scans obtained with 1–2 mm collimation (Ooi et al. 2003b; Bergin et al. 1986; Bégin et al. 1991; Mathieson et al. 1989; Remy-Jardin et al. 1990; Gevenois et al. 1994). These CT techniques allowed clearer depiction of nodules, pleural calcification and conglomeration of nodules than the chest radiograph. Due to superimposition of lesions, 7 mm or 10 mm conventional or spiral CT

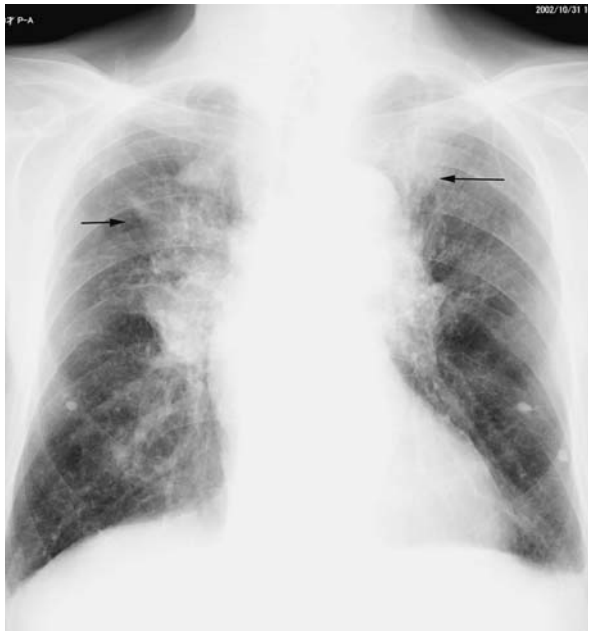

a

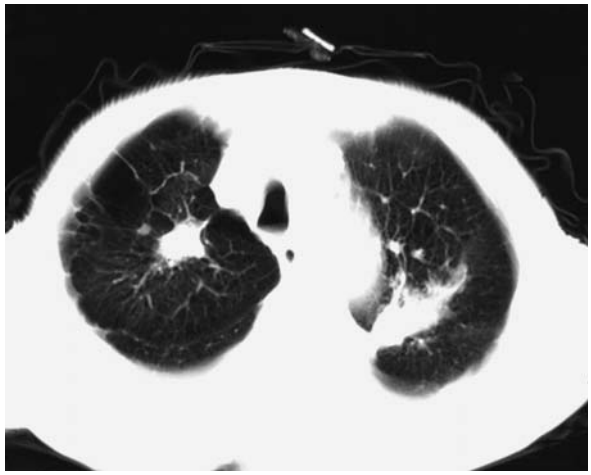

b

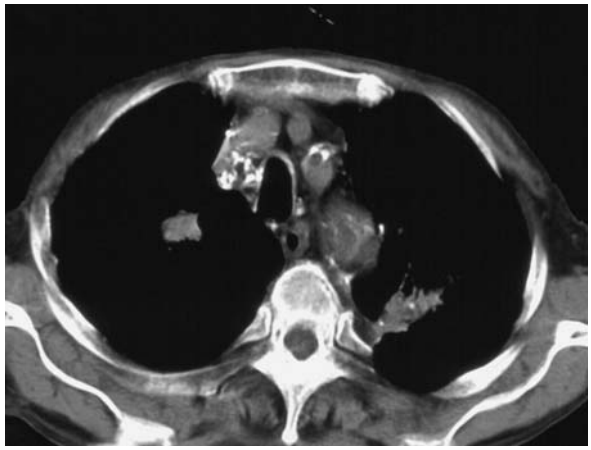

c

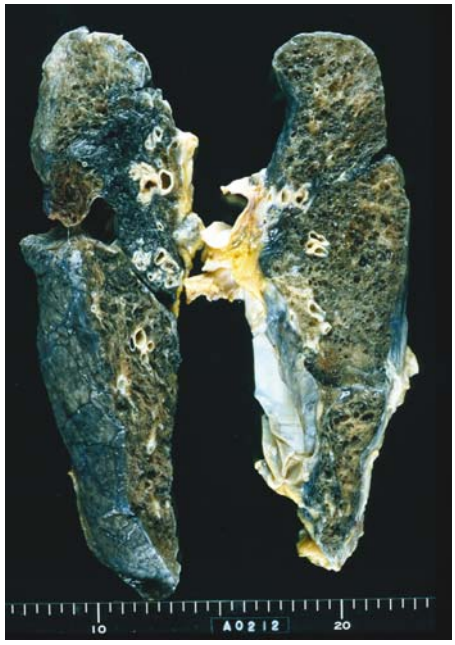

d

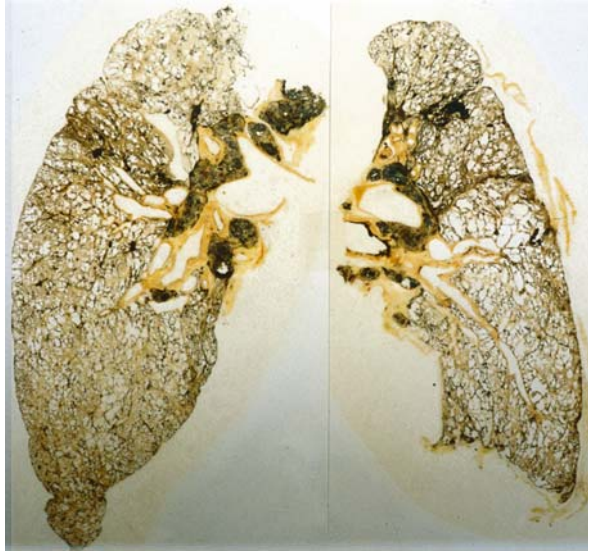

e

Fig. 5.5a–e. Complicated silicosis in a 79-year-old retired tunnel worker. **a** Posterior–anterior chest radiograph shows bilateral large opacities in the upper lung zones near the pulmonary hila (*arrows*) compatible with the diagnosis of complicated silicosis. Note that there is bilateral hilar lymphadenopathy with reduced background nodulation. **b** Spiral computed tomography image (10-mm thickness) shows bilateral larger nodules with irregular shape, suggesting progressive massive fibrosis (PMF). There are paracicatricial emphysema around the PMF in the right lung. **c** Mediastinal window image shows punctuate calcification in the PMF as well as in the mediastinal lymph nodes. **d** Macroscopic lung image in coronal section reveals black-pigmented PMF in the right upper lung zone adjacent to and contiguous with the right hilar lymphadenopathy. There is moderate centrilobular emphysema but sparse silicotic nodules. **e** Gough–Wentworth whole-lung section clearly demarcates the PMF as well as silicotic nodules with pigmentation. Note that there are advanced emphysematous changes around the PMF in both upper lobes

sections are advocated as the best technique to identify micronodules clustered around vascular structures (Mathieson et al. 1989), while thin-section CT is superior to the thicker conventional or spiral CT sections in imaging small nodules less than 1.5 mm with low attenuation that may be obscured by partial volume averaging in the latter CT techniques (Bégin et al. 1988, 1991).

The superiority and utility of thin-section CT in identifying nodules not seen on the chest radiograph or on conventional or spiral CT is illustrated in the study by Bégin et al. (1991). They studied 49 patients who had been exposed to silica dust in mines and foundries. All 49 had ILO chest radiograph scores of 0 or 1. Of the 49 patients, 32 had normal chest radiographs, 6 were categorized as having indeterminate chest radiographs and 13 had abnormal chest radiographs. Of the 32 patients with normal chest radiographs, 13 (41%) cases were identified using either CT or thin-section CT to have silicosis. In addition, a further 10% of cases were diagnosed to have silicosis only on the thin-section CT scan (Bégin et al. 1991).

Early confluence of nodules and emphysema that are not obvious on the chest radiograph can be demonstrated on conventional or spiral CT and thin-section CT (Ooi et al. 2003b; Bergin et al. 1986; Bégin et al. 1991) (Fig. 5.6). In a study of 76 men with silicosis, Ooi et al. determined that 26 had simple silicosis based on their chest radiographs; the remaining 50 men had radiographic evidence of PMF (Ooi et al. 2003b). Of the 26 men with radiographic evidence of simple silicosis, 10 (38.5%) were found to have early confluence of nodules greater than 1.5 cm, denoting PMF, on CT (Ooi et al. 2003b). A similar proportion (40%) of workers with PMF diagnosed on CT were also noted to have been under-represented on the chest radiograph in a separate study by Bégin et al. (1988).

Gevenois et al. studied the lungs of 40 coal miners without radiographic evidence of pneumoconiosis (ILO profusion score <1/0) with CT and thin-section CT (Gevenois et al. 1994). They noted that the combined technique was superior to either technique alone in the detection of pulmonary nodules. The combined technique identified micronodules in 16 of the 40 miners (40%) who were determined on the chest radiograph not to have pneumoconiosis. The combined CT technique, therefore, optimizes characterization and delineation of disease extent in silicosis and has been extensively evaluated by several workers in the study of pneumoconiosis (Ooi et al. 2003b; Bergin et al. 1986; Bégin et al. 1991; Mathieson et al. 1989; Remy-Jardin et al. 1990; Gevenois et al. 1994). However, with the advent of multi-slice CT, it is now possible to retrospectively reconstruct the acquired data into any slice thickness and algorithm necessary to evaluate the lungs in silicosis (Fig. 5.7).

On CT and thin-section CT, the silicotic nodules are well defined, ranging from 2 mm to 5 mm, and are found predominantly in the centrilobular and

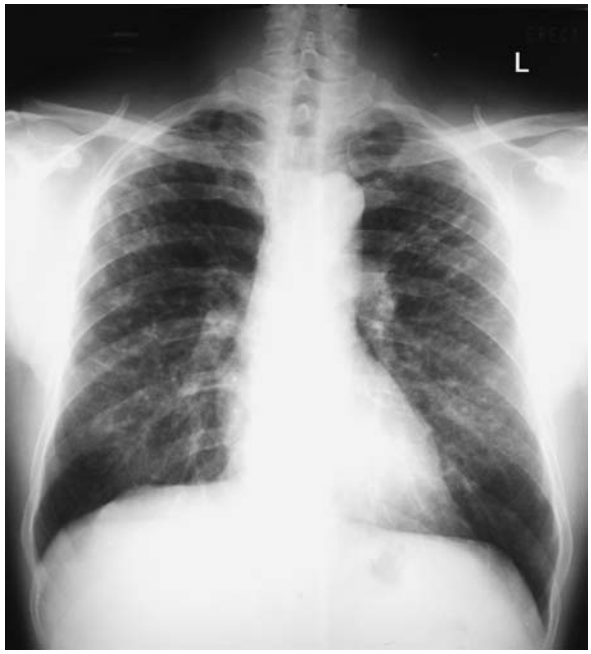

a

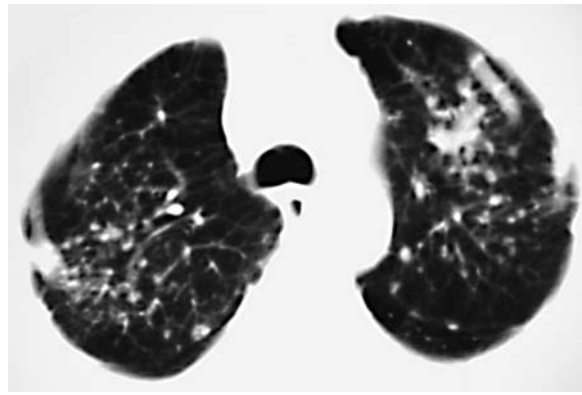

b

Fig. 5.6a,b. A 69-year-old retired construction site worker. **a** Posterior–anterior chest radiograph shows irregular nodular opacities in both upper- and mid-zones. **b** Spiral computed tomography (7-mm thickness) through the lung apices show early conglomeration of nodules, particularly on the left

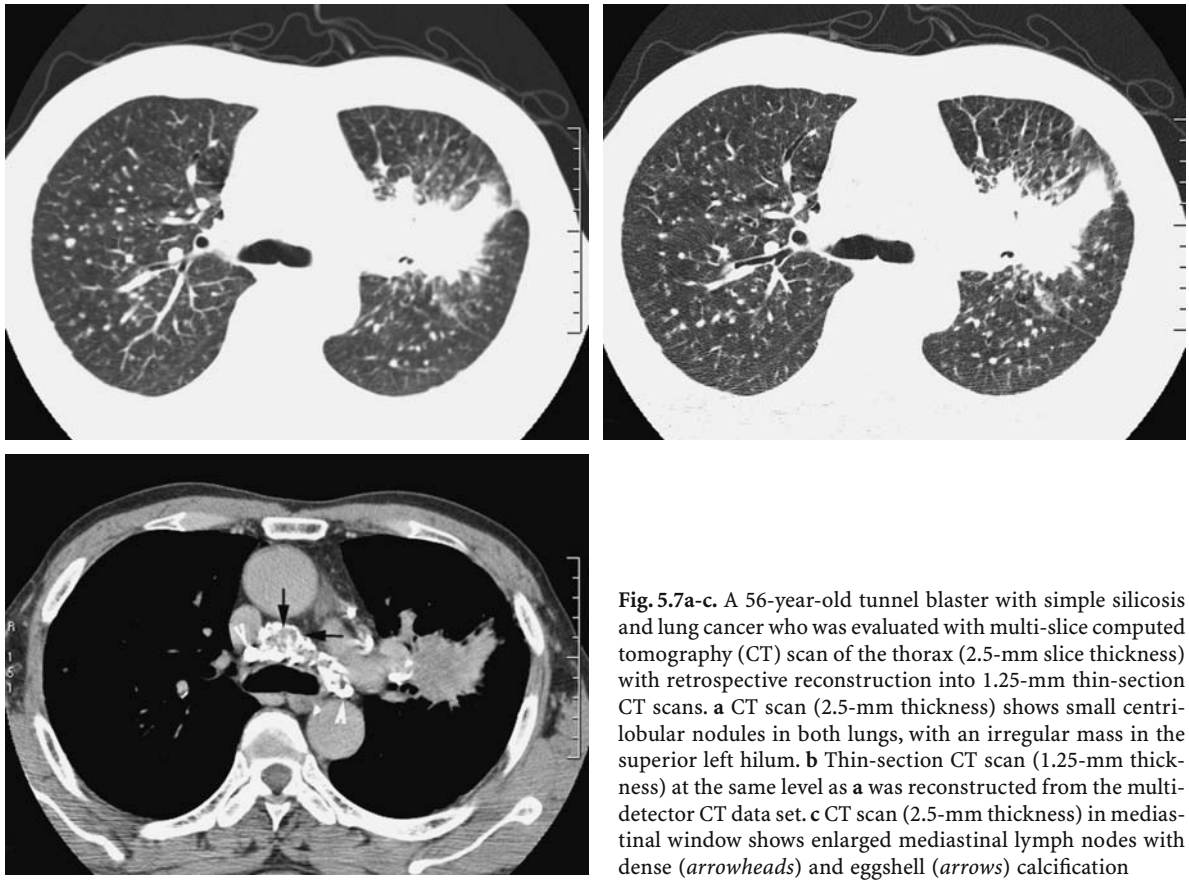

Fig. 5.7a-c. A 56-year-old tunnel blaster with simple silicosis and lung cancer who was evaluated with multi-slice computed tomography (CT) scan of the thorax (2.5-mm slice thickness) with retrospective reconstruction into 1.25-mm thin-section CT scans. **a** CT scan (2.5-mm thickness) shows small centrilobular nodules in both lungs, with an irregular mass in the superior left hilum. **b** Thin-section CT scan (1.25-mm thickness) at the same level as **a** was reconstructed from the multidetector CT data set. **c** CT scan (2.5-mm thickness) in mediastinal window shows enlarged mediastinal lymph nodes with dense (*arrowheads*) and eggshell (*arrows*) calcification

subpleural distribution (Fig. 5.1 and Fig. 5.8). Usually diffuse and bilateral with posterior lung dominance, the nodules in milder cases may be confined to the upper lobes, with sparing of the lower zones. Conglomerate masses or PMF appear as mass-like consolidation, usually with irregular margins and associated with adjacent paracicatricial emphysema and lung parenchymal architectural distortion (Fig. 5.5, Fig. 5.9 and Fig 5.10). The PMF lesions are usually found in the apical and posterior segments of the upper and lower lobes. Cavitation of the PMF lesions occurs as a result of ischemic necrosis or tuberculous infection (Fig. 5.9). Calcification when present may be punctuate, linear or massive (Akira 2002) (Fig. 5.5). Paracicatricial emphysema (Fig. 5.9, Fig. 5.10) has been observed to be more prominent in patients with silicosis compared with coal workers' pneumoconiosis (Remy-Jardin et al. 1990). In their review of thin-section CT scans in 55 patients with type-p pneumoconiosis, Akira et al. found intralobular areas of low attenuation with a central dot, which corresponded to irregular fibrosis around and along the respiratory bronchioles and to focal areas of centrilobular emphysema in two post-mortem specimens (Akira et al. 1989). Nevertheless, there is still debate whether centrilobular emphysema (Fig. 5.10) found in silicosis is due to silica dust per se, exposure to other dust, such as coal and asbestos, or to concomitant smoking (Bégin et al. 1991, 1995; Kinsella et al. 1990). Some studies have reported that emphysema in silicosis occurs independently of smoking (Gevenois et al. 1998; American Thoracic Society Committee of the Scientific Assembly of Environmental and Occupational Health 1997; Hnizdo et al. 1994), while other investigators believe that silicosis per se without PMF does not contribute to emphysema (Bégin et al. 1991, 1995; Akira et al. 1989; Kinsella et al. 1990; Gevenois et al. 1998).

Hilar and mediastinal lymph nodes are generally enlarged and may calcify. Ooi et al. reviewed CT scans of 41 men with silicosis for distribution and pattern of calcification of mediastinal lymph nodes in six lymph node stations (Ooi et al. 2003a). All patients had enlarged lymph nodes in at least two lymph node stations, with calcification found in nearly 50% of lymph node stations. Hyperdense lymph node (Fig. 5.8) was present in one-third of

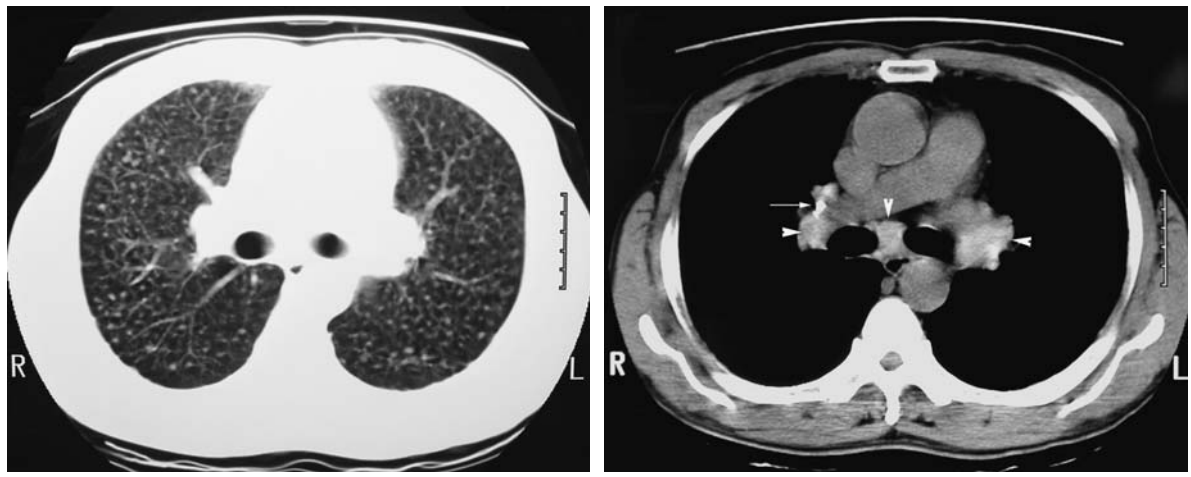

a b

Fig. 5.8a,b. A 78-year-old retired construction site worker. **a** Computed tomography (CT) scan (7-mm thickness) through the upper lobes shows typical silicotic nodules in a centrilobular distribution. **b** CT scan in mediastinal window shows densely calcified (*arrow*) and hyperdense (*arrowheads*) lymph nodes in the mediastinum and hila

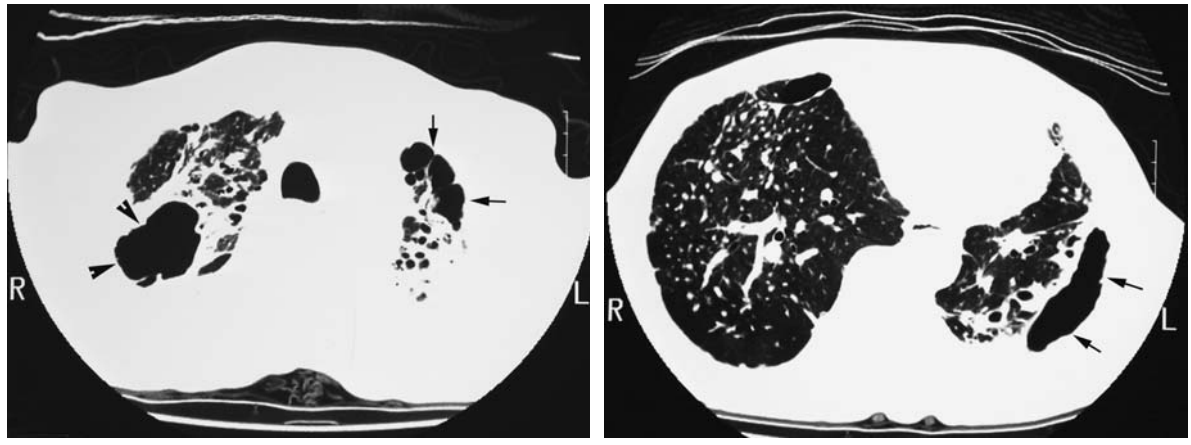

a b

Fig. 5.9a,b. A 74-year-old retired tunnel blaster with progressive massive fibrosis (PMF) complicated by tuberculosis. **a** Thin-section CT scan through the lung apices shows a cavitating PMF lesion (*arrowheads*) in the right upper lobe secondary to *mycobacterium tuberculosis* infection. Note paracicatricial emphysema (*arrows*) surrounding the left PMF lesion and traction bronchiectasis in both lung apices. **b** Thin-section CT scan through the lower lobes shows a loculated pneumothorax (*arrows*) at the lateral aspect of the left lower lobe secondary to ruptured paracicatricial emphysema

lymph node stations, most frequently in the subcarinal region. The predominant type of calcification was the uniformly dense calcified lymph node (53.4%) (Fig. 5.7 and Fig. 5.8) followed by the speckled variety (26.4%). Central, eccentric and eggshell calcification (Fig. 5.7) was rare (4.3, 7.7 and 5.2%, respectively).

Thin-section CT appearances of silicoproteinosis have been described only in occasional case reports (Marchiori et al. 2001). In addition to diffuse ground-glass opacities that typify idiopathic alveolar proteinosis, the presence of centrilobular poorly defined nodules and consolidation in the dorsal portion of lower lobes serve to differentiate silicoproteinosis from the former. Bilateral hilar lymphadenopathy is another discriminating feature found in silicoproteinosis. The pathological basis for the centrilobular nodules and peripheral consolidation has not been disclosed, although ground-glass opacity has been attributed to the accumulation of excess alveolar surfactant protein.

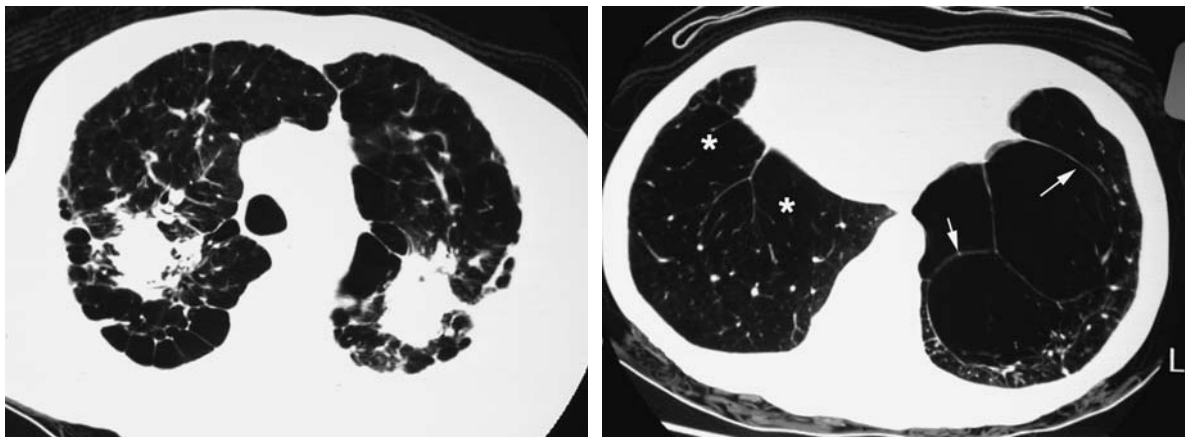

Fig. 5.10a,b. A 68-year-old retired construction site worker. **a** Thin-section CT scan through the upper lobes shows bilateral progressive massive fibrosis (PMF) with surrounding paracicatricial emphysema. **b** Thin-section CT scan through the lower lobes shows confluent centrilobular emphysema (*asterisks*) in the right lower lobes and bullae in the left lower lobe (*arrows*)

5.5.3 Radiological–Clinical Correlation Using CT Techniques

Most studies that have evaluated the utility of CT in silicosis have largely applied the ILO classification, with some modifications, to grade nodular profusion on CT (Bergin et al. 1986; Bégin et al. 1987, 1991, 1995; Kinsella et al. 1990; Ooi et al. 2003a; Talini et al. 1995). Although some previous studies have shown a poor relationship between nodular profusion and lung function (Bergin et al. 1986), other workers have described associations between deteriorating lung function and nodular profusion and coalescence, respectively (Ooi et al. 2003b; Bégin et al. 1988; Kinsella et al. 1990; Gevenois et al. 1998; Talini et al. 1995). Bégin et al. investigated the relationship between lung function, airflow limitation and lung injury assessed on the chest radiograph and CT scans in 94 silica-exposed workers in the foundry and granite industries (Bégin et al. 1988). Workers who had radiographic or CT evidence of coalescence of nodules and conglomerate masses had significant reductions in lung volume, impaired gas exchange and airflow obstruction compared with their counterparts who did not show lung function impairment.

In their study on 17 patients with silicosis and 6 controls, Bergin et al. graded CT scans for nodular profusion and extent of emphysema and measured mean lung attenuation (Bergin et al. 1986). Although there was a significant correlation between ILO radiographic scores of nodular profusion and mean lung attenuation and visual CT scores, there was poor correlation between radiographic and CT scores of nodular profusion and lung function. There was, however, a significant relationship between extent of emphysema graded on CT and indices of airflow obstruction ($r>0.66$, $P<0.001$) and diffusing capacity ($r=0.71$, $P<0.001$).

Emphysema in silicosis can arise from a number of factors, including cigarette smoking, exposure to silica and other dusts such as coal and asbestos and the presence of PMF, as discussed above. To address this issue, Kinsella et al. stratified 30 silica exposed workers into two groups: one group comprised 18 workers who were ex-smokers or current smokers, and the second group consisted of 12 workers who were lifetime non-smokers (Kinsella et al. 1990). Comparison was made between the two groups with respect to extent of emphysema and nodules, respectively, on CT. Extent of emphysema was the strongest independent predictor of lung function impairment, while extent of nodules was a weaker independent predictor of diffusing capacity only. This study also showed that in the absence of PMF, smokers had worse emphysema and lung-function impairment than non-smokers. There was no such difference in the group with PMF. The authors, in agreement with other investigators, concluded that in the absence of PMF, silicosis was not associated with significant emphysema (Bégin et al. 1991, 1995; Akira et al. 1989; Kinsella et al. 1990; Gevenois et al. 1998).

In 2003, Ooi et al. further explored the relationship between nodular profusion, PMF, emphysema and lung function in 76 silica-exposed men (Ooi et al. 2003b). Nodular profusion on CT was evalu-

ated visually and also quantitatively by application of attenuation threshold to isolate areas of attenuation greater than -100 HU. Mean lung density was also obtained and emphysema quantified using an attenuation threshold less than -950 HU. Visual and quantitative CT parameters of nodular profusion and extent of PMF and emphysema showed inverse relationships with lung function indices: the correlation coefficients ranged from 0.47 to 0.63, (P<0.001) and 0.41 to 0.61 (P<0.001) for FEV_1 and FEV_1/FVC, respectively. Chest radiograph scores for nodular profusion showed similar relationships to indices of obstruction, albeit with lower correlation coefficients. After multiple regression, extent of PMF and emphysema remained significant independent determinants of FEV_1 and FEV_1/FVC, while mean lung attenuation was an independent predictor of lung volume and diffusing capacity. Smoking and duration of silica exposure exerted no independent effects on lung function. Although there were no significant differences with respect to age, duration of silica exposure and cigarette consumption among workers with simple silicosis and PMF, those with PMF had significantly impaired lung function and higher radiological scores compared with their counterparts. Abnormal FEV_1 and FVC (<70% predicted) were also observed in one-third of workers with simple silicosis, consistent with the result of a recent meta-analysis that found an association between silica exposure and airflow obstruction, even in non-smokers (American Thoracic Society Committee of the Scientific Assembly of Environmental and Occupational Health 1997; Hnizdo et al. 1994; Oxman et al. 1993; Becklake et al. 1987).

Ooi et al. also evaluated the relationship between mediastinal lymph node attenuation with severity of nodular profusion and PMF on CT and lung function in 41 men with silica exposure. Increasing lymph node attenuation was directly related to severity of nodular profusion and PMF and inversely related to diffusion coefficient (Ooi et al. 2003a). Men with more severe nodular profusion also had a greater number of calcified lymph node stations, while men with larger numbers of calcified lymph node stations had significantly reduced diffusion coefficients compared with those with fewer calcified lymph node stations. These relationships imply that mediastinal lymph nodes in silicosis increase in attenuation and calcification with severity of lung disease and functional impairment and concur with the findings of Friedetzky et al., who determined that changes in lymph nodes occurred in tandem with lung changes in rats induced with silicosis (Friedetzky et al. 1998). Similar associations between dust-related changes in the hilar lymph nodes and pneumoconiotic lung disease were also found in a post-mortem study of 123 coalminers (Seal et al. 1986). Release of dust-laden macrophages from rupture of necrotic collagenous material from affected lymph nodes into adjacent bronchus or pulmonary arterial branch have been postulated to perpetuate the cycle of inflammation and fibrosis in silicosis (Seal et al. 1986). Impaired lymphatic clearance may be an alternative mechanism to explain these associations between hilar lymph nodes and pneumoconiotic lung changes.

5.6 Complications

There are a few diseases that may complicate silicosis; these are primarily Caplan's syndrome, tuberculosis, carcinoma and connective tissue disease. The two most serious complications, lung cancer and tuberculosis, may affect the prognosis and natural history of the underlying disease.

Caplan's syndrome, also known as rheumatoid pneumoconiosis, was initially identified in coal workers' pneumoconiosis but is now known to occur in silicosis as well (Honma and Vallyathan 2002). The incidence of this disease ranges from 0.48% to 0.74% (Honma and Vallyathan 2002). The rheumatoid pneumoconiotic nodules are similar to necrobiotic nodules seen in rheumatoid arthritis and are described as either classic or silicotic type based on their pathological findings (Honma and Vallyathan 2002). The classic type corresponds to the original Caplan's cases, showing large nodules characterized by uniform necrosis and associated with little background pneumoconiotic nodules. The silicotic type consists of multiple smaller nodules, with the necrotic area retaining some characteristics of a silicotic nodule. In both types, a layer of palisaded inflammatory cells surrounds the peripheral zone of the nodules. On the chest radiograph, rheumatoid pneumoconiosis presents with multiple well-defined nodules ranging from 5 mm to 5 cm distributed throughout both lung fields with peripheral predominance (Caplan 1953). Characteristically, these nodules appear suddenly within a few months during the follow-up of those patients. On CT, the rheumatoid pneumoconiotic nodules are well defined and may cavitate and calcify (Arakawa

et al. 2003). However, it may be impossible to distinguish silicotic-type nodules of rheumatoid pneumoconiosis from silicotic nodules per se.

It is well established that silicosis predisposes to tuberculous infection, although this predisposition is dependent on the prevalence of tuberculosis in the population from which the workers originate (Becklake 1992). Workers with more severe disease in terms of nodular profusion and PMF are at greatest risk of acquiring tuberculosis, which in turn is associated with an increased likelihood of radiographic progression (Lee et al. 2001). Cavitation of PMF lesions (Fig. 5.9), unusually rapid advancement in nodular profusion or size and presence of tree-in-bud opacities on CT, indicating endobronchial infection, are pointers to the development of silicotuberculosis (Lee and Im 1995; Kuhlman et al. 1994; Solomon 2001). In cases of indolent nodular tuberculosis, it may be impossible to isolate the tubercle bacilli in the sputum, in which case polymerase chain reaction has been advocated as a means of identifying the organism (Cheng et al. 1993).

The association between silicosis and lung cancer is also well documented. Silica has been recognized as a probable human carcinogen [International Agency for Research on Cancer (IARC) type 2A] since 1987 (IARC monographs; 1987). In 1997 (IARC monographs; 1997) the classification of silica was changed from 2A (probable human carcinogen) to type 1 (known human carcinogen). The risk is greatest for workers with established silicosis compared with those with silica exposure, who have a reduced albeit still elevated risk of lung cancer (Chiyotani et al. 1990; Smith et al. 1995; Tsuda et al. 2002).

The strength of the association between silicosis and connective tissue disease varies with the type of connective tissue disorder. The risk of developing systemic sclerosis, particularly in workers with high exposure to silica dust, is well established, although such casual associations between silicosis, rheumatoid arthritis and systemic lupus erythematosis are less widely reported (Rosenman 1999; Sluis-Cremer et al. 1985, 1986; Sanchez-Roman et al. 1993)

5.7 Differential Diagnosis

A similar centrilobular and subpleural distribution of nodules may be noted in sarcoidosis and lymphangitis carcinomatosis, although a careful review of the clinical history may provide useful pointers for and against these other diseases. In addition, on thin-section CT, there are a few distinguishing features, such as beaded septa and fissures and reticular opacities, which are usually not found in silicosis. Clustering of nodules around parahilar regions and bronchi are also more commonly found with sarcoidosis.

5.8 Future Developments

Despite the considerable debate over the role of emphysema, nodule coalescence and PMF in the development of airflow obstruction in silicosis, the ILO classification does not provide classification of emphysema, although it recognizes the presence of bulla, which it denotes as "bu" (Geneva, International Labor Office 2000). There is, however, no system for quantifying bullous change. The chest radiograph is also significantly insensitive in evaluating the extent or severity of emphysema in comparison with CT and thin-section CT, which are techniques that allow quantification of severity and extent of both emphysema and lung nodules. There is also no current consensus on the size of PMF in the pneumoconiosis. Although the ILO radiographic classification recognizes the presence of PMF when a single opacity in the radiograph exceeds 1 cm in diameter (Geneva, International Labor Office 2000; Bégin et al. 1988), the College of American Pathologists defines PMF in coal workers pneumoconiosis as lesions larger than 2 cm (Gamsu 1991; Kleinerman et al. 1979).

There is, therefore, a need for a standardized, reproducible and internationally accepted CT/thin-section CT classification system for the pneumoconiosis in the English language, such as the ILO classification for the chest radiograph. There has been a recent multi-center study involving an international panel of experts who have applied a coding sheet for CT/thin-section CT lung appearances developed by a task group on Diagnostic Radiology in Occupational and Environmental Diseases (Hering 2004; Hering and Kraus 2005). This coding sheet is a descriptive classification of CT and thin-section CT appearances of parenchymal and pleural abnormalities found in occupational and environmentally related diseases. In this system, not only is the presence of each abnormality found in each lung zone and the pleura described, but also, at the

same time, the severity and extent of silicotic nodules, PMF, diffuse interstitial fibrosis (i.e., reticular opacities and ground-glass opacity) and emphysema are quantified based on the reference images. The establishment of a reproducible CT/thin-section CT classification system would, therefore, standardize the reporting and documentation of abnormalities found in the CT/thin-section CT evaluation of pneumoconiosis.

Other imaging techniques that are currently available to evaluate the chest include magnetic resonance imaging (MRI) and positron emission tomography (PET), although the utility of both techniques has not been substantially evaluated or validated in silicosis. Matsumoto et al. evaluated MR appearances in 17 patients with 34 PMF lesions, 11 of whom had silicotuberculosis (Matsumoto et al. 1998b). They classified signal intensity pattern on T1- and T2-weighted images (WI) and the pattern of contrast enhancement. The most common signal change of PMF lesions was isointensity (70%) on T1-WI and hypointensity (68%) on T2-WI relative to skeletal muscle. In 41% of lesions, focal hyperintense areas were noted within the PMF lesions, which corresponded to low density areas on CT, suggestive of necrosis. Rim enhancement was present in a little over half (53%) of all cases. Diffuse enhancement was noted in only 2 of 34 PMF lesions; the remaining lesions did not enhance reflecting the hypovascular nature of the hyaline collagenous tissue without formation of new capillaries or cellular reaction that comprise PMF lesions in silicosis (Spencer 1985). The authors hypothesized that the rim enhancement described above was due to collapsed alveoli caused by emphysema (Matsumoto et al. 1998b). The same authors also described MRI features of lung cancer occurring in a patient with PMF (Matsumoto et al. 1998a) as a high-signal intensity area separate from the fibrotic mass, which appeared as a low-signal intensity area, on both T1- and T2-weighted images. MRI, particularly with gadolinium enhancement, may therefore be potentially useful in differentiating lung cancer from the fibrous tissue in the PMF lesions. Other uses of MRI may lie in imaging complications of silicosis that involve the central vessels, such as pulmonary artery stenosis, with MR angiography being a less invasive modality than conventional angiography (Mahnaken et al. 2001).

The utility of PET-CT in silicosis has not been thoroughly investigated, but increased uptake has been described in both PMF lesions and also in enlarged mediastinal and hilar lymph nodes in silicosis (O'Connell and Kennedy 2004) (Fig. 5.11). Whether this will present problems when there is a concomitant lung cancer arising in a silicosis patient, particularly one complicated by PMF, remains unclear, although Bandoh et al. have described the utility of PET in identifying malignancy in the set-

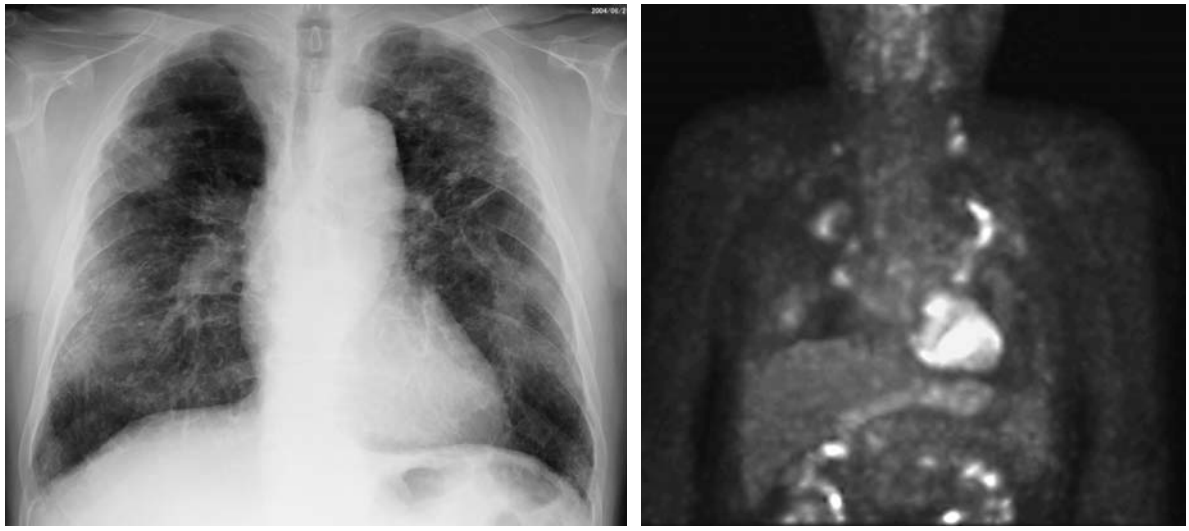

Fig. 5.11a,b. A 71-year-old retired metal ore miner. **a** Chest radiograph shows multiple conglomerated masses in both upper and lower lobes with diffuse pleural thickening adjacent to the masses bilaterally. Silicotic nodules are also present especially around the masses. **b** F-18 Fluorodeoxyglucose (FDG) positron emission tomography image with maximum intensity projection shows increased uptake of FDG in the progressive massive fibrosis lesions. The high uptake in the upper lobe lesions is indistinguishable from that of pulmonary neoplasm. The uptake in the lower lobe lesions is less prominent. Weak uptake is also identified in bilateral hilar lymph nodes and left supraclavicular node

ting of pneumoconiosis (Bandoh et al. 2003). A new PET tracer, a fluorinated analog of proline amino acid, cis-4-[(18)F]fluoro-L-proline (FP), was tested for potential use in PET for detection and evaluation of pulmonary response to respirable crystalline silica in experimental rabbits (Wallace et al. 2003). The results were promising, with increased uptake noted in the lungs of silicotic animals compared with controls. This suggests that FP PET imaging may have the potential sensitivity to detect active fibrosis in silicosis and other lung diseases.

References

Absher MP, Hemenway DR, Leslie KO et al (1992) Intrathoracic distribution and transport of aerosolized silica in the rat. Exp Lung Res 18:743-757

Akira M (2002) High resolution CT in the evaluation of occupational and environmental disease. Radiol Clin North Am 40:43-59

Akira M, Higashihara T, Yokoyama K et al (1989) Radiographic type p pneumoconiosis: high-resolution CT. Radiology 171:117-123

American Thoracic Society Committee of the Scientific Assembly of Environmental and Occupational Health (1997) Adverse effects of crystalline silica exposure. Am J Respir Crit Care Med 155:761-765

Arakawa H, Honma K, Shida H et al (2003) Computed tomography findings of Caplan syndrome. J Comput Assist Tomogr 27:758-760

Bailey WC, Brown M, Buechner HA et al (1974) Silico-mycobacterial disease in sandblasters. Am Rev Respir Dis 110:115-125

Bandoh S, Fujita J, Yamamoto Y et al (2003) A case of lung cancer associated with pneumoconiosis diagnosed by fluorine-18 fluorodeoxyglucose positron emission tomography. Ann Nucl Med 17:597-600

Becklake MR (1992) The mineral dust diseases. Tuber Lung Dis 73:13-20

Becklake MR, Irwig L, Kielkowski D et al (1987) The predictors of emphysema in South African gold miners. Am Rev Respir Dis 135:1234-1241

Bégin R, Bergeron D, Samson L et al (1987) CT assessment of silicosis in exposed workers. Am J Roentgenol 148:509-514

Bégin R, Ostiguy G, Cantin A et al (1988) Lung function in silica-exposed workers. A relationship to disease severity assessed by CT scan. Chest 94:539-545

Bégin R, Ostiguy G, Fillion R et al (1991) Computed tomography in the early detection of silicosis. Am Rev Respir Dis 44:697-705

Bégin R, Filion R, Ostiguy G (1995) Emphysema in silica- and asbestos-exposed workers seeking compensation. A CT scan study. Chest 108:647-655

Bergin CJ, Müller NL, Vedal S et al (1986) CT in silicosis: correlation with plain films and pulmonary function tests. Am J Roentgenol 146:477-483

Bitterman PB, Rennard SI, Adelberg S et al (1983) Role of fibronectin as a growth factor for fibroblasts. J Cell Biol 97:1925-1932

Brown GP, Monicj M, Hunninghake GW (1988) Fibroblast proliferation induced by silica-exposed human alveolar macrophages. Am Rev Respir Dis 138:85-89

Buechner HA, Ansari A (1969) Acute silico-proteinosis. A new pathologic variant of acute silicosis in sandblasters, characterized by histologic features resembling alveolar proteinosis. Dis Chest 55:274-278

Caplan A (1953) Certain unusual radiological appearances in the chest of coal-miners suffering from rheumatoid arthritis. Thorax 8:29-37

Cheng SJ, MA Y, Pan YX (1993) A study on the diagnosis of pulmonary tuberculosis and silicotuberculosis by PCR. Zhonghua Jie He He Hu Xi Za Zhi 16:221-224

Chiyotani K, Saito K, Okubo T et al (1990) Lung cancer risk among pneumoconiosis patients in Japan, with special reference to silicotics. IARC Sci Publ 97:95-104

Corry D, Kulkarni P, Lipscomb MF (1984) The migration of bronchoalveolar macrophages into hilar lymph nodes. Am J Pathol 115:321-328

Davies D (1974) Disability and coal workers pneumoconiosis. BMJ 2:652

Davis GS, Gemsa D (1996) Immunopathogenesis of silicosis. In: Immunopathology of lung disease. Edited by Kradin RL and Robinson BWS. Butterworth-Heinemann, Oxford, pp 445-467

Dees PM, Suratt P, Winn W (1978) The radiographic finding in acute silicosis. Radiology 126:359

Dubois CM, Bissonnette E, Rola-Pleszczynski M (1989) Asbestos fibers and silica particles stimulate rat alveolar macrophages to release tumour necrosis factor. Autoregulatory role of leukotriene B4. Am Rev Respir Dis 139:1257-1264

Elmes PC (1994) Inorganic dusts. In: Raffle PAB, Adams PH Baxter PJ, Lee WR (eds) Hunter's diseases of occupations, 8th edn. Arnold, London

Engholm G, von Schamlensee G (1982) Bronchitis and exposure to manmade mineral fibers in nonsmoking construction workers. Eur J Respir Dis [Suppl] 118:73-88

Epler GR, McCloud TC, Gaensler EA et al (1978) Normal chest roentgenogtrams in chronic diffuse infiltrative lung disease. N Engl J Med 298:943-939

Epstein DM, Miller WO, Bresnitz EA et al (1984) Application of ILO classification to a population without industrial exposure: findings to be differentiated from pneumoconiosis. AJR 142:53-58

Friedetzky A, Garn H, Kirchner A et al (1998) Histopathological changes in enlarged thoracic lymph nodes during the development of silicosis in rats. Immunobiology 199:119-132

Gamsu G (1991) Computed Tomography and High Resolution Computed Tomography of Pneumoconioses. Journal of Occupational Medicine 33:794-796

Geneva, International Labor Office (2000) International Labor Office Guidelines for the use of ILO International Classification of Radiographs of Pneumoconiosis. Occupational safety and health series no 22

Gevenois PA, Pichot E, Dargent F et al (1994) Low grade coal worker's pneumoconiosis. Comparison of CT and chest radiography. Acta Radiol 35:351-356

Gevenois PA, Sergent G, de Maertelaer V et al (1998) Micronodules and emphysema in coal mine dust or silica exposure: relation with lung function. Eur Respir J 12:1020-1024

Gibbs AR, Wagner JC (1998) Disease due to Silica. In: Churg A,

Green FHY, (eds) Pathology of occupational lung disease, 2nd edn. Williams and Wilkins, Baltimore, pp 209-234
Graham WH (1992) Silicosis. Clin Chest Med 13:253-267
Gross BH, Schneider HJ, Protos AV (1980) Eggshell calcification of lymph nodes: an update. Am J Roentgenol 135:1265-1268
Gupta BN, Rastogi SK, Husain T et al (1991) A study of respiratory morbidity and pulmonary function among solderers in the electronics industry. Am Ind Hyg Assoc J 52:45-51
Hansell DM, Kerr IH (1991) The role of high resolution computed tomography in the diagnosis of interstitial lung disease. Thorax 46:77-84
Harmsen AG, Muggenburg BA, Snipes MB et al (1985) The role of macrophages in particle translocation from lungs to lymph nodes. Science 230:1277-1280
Heppleston AG, Young AE (1972) Alveolar lipo-proteinosis: an ultrastructural comparison of the experimental and human forms. J Pathol 107:107-117
Hering KG (2004) Standardized CT/HRCT-classification of the German Federal Republic for work and environmental related thoracic diseases. Radiologe 44:500-511
Hering KG, Kraus T (2005) Coding CT-Classification in Occupational and environmental respiratory diseases. In Kusaka Y, Hering KG, Parker JE (eds) International classification of HRCT for occupational and environmental respiratory diseases. Springer, Berlin Heidelberg New York
Hnizdo E, Sluis-Cremer GK, Baskind E et al (1994) Emphysema and airway obstruction in non-smoking South African gold miners with long exposure to silica dust. Occup Environ Med 51:557-563
Hoffmann EO, Lamberty J, Pizzolato P et al (1973) The ultrastructure of acute silicosis. Arch Pathol 96:104-107
Honma K, Vallyathan V (2002) Rheumatoid pneumoconiosis: a comparative study of autopsy cases between Japan and North America. Ann Occup Hyg 46S:265-267
Honma K, Abraham JL, Chiyotani K et al (2004) Proposed criteria for mixed-dust pneumoconiosis: definition, descriptions, and guidelines for pathologic diagnosis and clinical correlation. Hum Pathol 35:1515-1523
Hughes JM, Jones RN, Gilson JC et al (1982) Determinants of progression in sandblasters' silicosis. Ann Occup Hyg 26:701-712
Hunninghake GW, Hemken C, Brady M et al (1986) Immune interferon is a growth factor for human lung fibroblasts. Am Rev Respir Dis 134:1025-1028
IARC Monographs on the evaluation of the carcinogenic risks of chemicals to humans, silica and some silicates (1987) Volume 42, IARC, Lyon, France
IARC Monographs on the evaluation of carcinogenic risks to humans (1997) Volume 68, IARC, Lyon, France
Jacobs LG, Gerstl B, Hollander AG et al (1956) Intraabdominal egg-shell calcification due to silicosis. Radiology 67:527-530
Jacobson G, Felson B, Pendergrass EP et al (1967) Egg shell calcification in coal and metal workers. Semin Roentgenol 2:276-281
Jagirdar J, Bégin R, Dufresne A et al (1996) Transforming growth factor-b in silicosis. Am J Respir Crit Care Med 154:1076-1081
Jiang CQ, Xiao LW, Lam TH et al (2001) Accelerated silicosis in workers exposed to agate dust in Guangzhou, China. Am J Ind Med 40:87-91
Johnson A, Moira CY, Maclean L et al (1985) Respiratory abnormalities among workers in an iron and steel foundry. Br J Ind Med 42:94-100
Jorgensen HS (1986) Silicosis in the iron-ore mine in Kiruna, Sweden, and the future need for silicosis control. Arch Occup Environ Health 58:251-257
Kampschimdt RF, Worthingrton ML, Mesecher MI (1986) Release of interleukin-1 (IL-1) and IL-1-like factors from rabbit macrophages with silics. J Leukoc Biol 39:123-132
Kinsella M, Müller N, Vedal S et al (1990) Emphysema in silicosis. A comparison of smokers with nonsmokers using pulmonary function testing and computed tomography. Am Rev Respir Dis 141:1497-1500
Kipen HM, Lilis R, Suzuki Y et al (1987) Pulmonary fibrosis in asbestos insulation workers with lung cancer. A radiological and histopathological evaluation. Br J Ind Med 44:96-100
Kleinerman J, Green F, Harley RA et al (1979) Pathology standards for coal worker's pneumoconiosis. Arch Pathol Lab Med 103:375-432
Koskinen H (1985) Symptoms and clinical findings in patients with silicosis. Scand J Environ Health 11:101-106
Kuhlman JE, Deutsch JH, Fishman EK, Siegelman SS (1990) CT features of thoracic mycobacterial disease. Radiographics. 10:413-431
Landrigan PJ, Cherniack MG, Lewis FA et al (1986) Silicosis in a grey iron foundry. The persistence of an ancient disease. Scand J Work Environ Health 12:32-39
Lauweryns JM, Baert JH (1977) Alveolar clearance and the role of pulmonary lymphatics. Am Rev Respir Dis 115:625-683
Lee HS, Poon WH, Ng TP (2001) Radiological progression and its predictive risk factors in silicosis. Occup Environ Med 58:467-471
Lee KS, Im JG (1995) CT in adults with tuberculosis of the chest. Characteristic findings and role in management. Am J Roentgenol 164:1361-1367
Lehnert BE, Valdez YE, Stewart CC (1986) Translocation of particles to the tracheobronchial lymph nodes after lung deposition: kinetics and particle-cell relationships. Exp Lung Res 10:245-266
Liddell FDK (1963) An experiment in film reading. Br J Ind Med 20:300
Liddell FDK, Lindars DC (1969) An elaboration of the ILO classification of simple pneumoconiosis. Br J Ind Med 26:89
Lugano EM, Dauber JH, Elias JA et al (1984) The regulation of lung fibroblast proliferation by alveolar macrophages in experimental silicosis. Am Rev Respir Dis 129:767-771
Mahnaken AH, Breuer C, Haage P (2001) Silicosis-induced pulmonary artery stenosis: demonstration by MR angiography and perfusion MRI. Br J Radiol 74:859-861
Marchiori E, Ferreira A, Muller NL (2001) Silicoproteinosis: high-resolution CT and histologic findings. J Thorac Imaging 16:127-129
Mathieson JR, Mayo JR, Staples CA et al (1989) Chronic diffuse infiltrative lung disease: comparison of diagnostic accuracy of CT and chest radiography. Radiology 171:111-116
Matsumoto S, Miyake H, Oga M et al (1998a) Diagnosis of lung cancer in a patient with pneumoconiosis and progressive massive fibrosis using MRI. Eur Radiol 8:615-617
Matsumoto S, Mori H, Miyake H et al (1998b) MRI signal characteristics of progressive massive fibrosis in silicosis. Clin Radiol 53:510-514

Michel RD, Morris JF (1964) Acute Silicosis. Arch Intern Med 113:850-855
Miller BG, Hagen S, Love RG et al (1998) Risks of silicosis in coal workers exposed to unusual concentrations or respirable quartz. Occup Environ Med 55:52-58
Muller NL, Mawson JB, Mathieson JR et al (1989) Sarcoidosis: correlation of extent of disease at CT with clinical, functional, and radiographic findings. Radiology 171:613-618
Murray J, Reid G, Kielkowski D et al (1993) Cor pulmonale and silicosis: a necropsy based case control study. Br J Ind Med 50:544-548
Nagelschmidt G (1960) The relation between lung dust and lung pathology in pneumoconiosis. Br J Ind Med 17:247-259
Neukirch F, Cooreman J, Korobaeff M et al (1994) Silica exposure and chronic airflow limitation in pottery workers. Arc Environ Health 49:459-464
Ng TP, Allan WG, Tsin TW et al (1985) Silicosis in jade workers. Br J Ind Med 42:761-764
Ng TP, Chan Sl, Lam KP (1987) Radiographic progression and lung function in silicosis: a ten year follow up study. BMJ 295:164-168
Nozaki S, Sawada Y (1959) Progress of simple pulmonary silicosis in retired miners. Jpn J Clin Tuberc 18:154
O'Connell M, Kennedy M (2004) Progressive massive fibrosis secondary to pulmonary silicosis appearance on F-18 fluorodeoxyglucose PET/CT. Clin Nucl Med 29:754-755
Oleru UG (1987) Respiratory and nonrespiratory morbidity in a titanium oxide paint factory in Nigeria. Am J Ind Med 12:173-180
Ooi GC, Ngan H, Peh WC et al (1997) Systemic lupus erythematosus patients with respiratory symptoms: the value of HRCT. Clin Radiol 52:775-781
Ooi CG, Khong PL, Cheng RS et al (2003a) The relationship between mediastinal lymph node attenuation with parenchymal lung parameters in silicosis. Int J Tuberc Lung Dis 7:1199-1206
Ooi GC, Tsang KWT, Cheung TF et al (2003b) Qualitative and quantitative CT evaluation in 76 men with silicosis: a clinical radiological correlative study. Radiology 228:816-825
Oxman AD, Muir DCF, Shannon HS et al (1993) Occupational dust exposure and chronic obstructive pulmonary disease. Am Rev Respir Dis 148:38-48
Rees D, Cronje R, du Toit RS (1992) Dust exposure and pneumoconiosis in a South African pottery. 1. Study objectives and dust exposure. Br J Ind Med 49:459-464
Remy-Jardin M, Degreef JM, Beuscart R et al (1990) Coal worker's pneumoconiosis: CT assessment in exposed workers and correlation with radiographic findings. Radiology 177:363-371
Rockoff SD, Schwartz A (1988) Roentgenographic underestimation of early asbestosis by International Labor Organization classification. Chest 93:108-109
Roeslin N, Lassabe-Roth C, Morand G et al (1980) La siilicoproteinose aique. Arch Mal Prof 41:15-18
Rosenmen KD, Moore-Fuller M, Reilly MJ (1999) Connective tissue disease and silicosis. Am J Ind Med 35:375-381
Saiyed HN, Chatterjee BB (1985) Rapid progression of silicosis in slate pencil workers. II. A follow up study. Am J Ind Med 8:135-142
Sanchez-Roman J, Wichmann I, Salaberri J et al (1993) Multiple clinical and biological autoimmune manifestations in 50 workers after occupational exposure to silica. Ann Rheum Dis 52:534-538
Schmidt JA, Oliver CN, Lepe-Zuniga JL et al (1984) Silica-stimulated monocytes release fibroblast proliferation factors identical to interleukin 1. A potential role for interleukin 1 in the pathogenesis of silicosis. J Clin Invest 73:1462-1472
Seal RME, Cockcroft A, Kung I et al (1986) Central lymph node changes and progressive massive fibrosis in coalworkers. Thorax 41:531-537
Sluis-Cremer GK, Hessel PA, Nizdo EH et al (1985) Silica, silicosis, and progressive systemic sclerosis. Br J Ind Med 42:838-843
Sluis-Cremer GK, Hessel PA, Hnizdo E et al (1986) Relationship between silicosis and rheumatoid arthritis. Thorax 41:596-601
Smith AH, Lopipero PA, Barroga VR (1995) Meta-analysis of studies of lung cancer among silicotics. Epidemiology 6:617-624
Solomon A (2001) Silicosis and tuberculosis, part 2. A radiographic presentation of nodular tuberculosis and silicosis. Int J Occup Environ Health 7:54-57
Spencer H (1985) Pathology of the lung: the Pneumoconiosis and other occupational lung diseases. Pergamon, Oxford
Talini D, Paggiaro PL, Falaschi F et al (1995) Chest radiography and high resolution computed tomography in the evaluation of workers exposed to silica dust: relation with functional findings. Occup Environ Med 52:262-267
Theron CP, Walters LG, Webster I (1964) The international classification of radiographs of the pneumoconiosis: Based on the findings in 100 decreased white South African gold miners: an evaluation. Med Proc (Johannesburg) 10:352
Tsuda T, Mino Y, Babazono A et al (2002) A case-control study of lung cancer in relation to silica exposure and silicosis in a rural area in Japan. Ann Epidemiol 12:285-287
Wallace WE, Gupta NC, Hubbs AF (2003) Cis-4-[F-18] fluoro-L-proline PET imaging of pulmonary fibrosis in a rabbit model. J Nucl Med 44:43-44
Weill H, Jones RN, Parkes WR (1994) Silicosis and related diseases. In: Parkes WR (ed) Occupational lung disorders, 3rd edn. Butterworth-Heinemann, Oxford, pp 285-339
White NW, Chetty R, Bateman ED (1991) Silicosis among gemstone workers in South Africa: tiger's-eye pneumoconiosis. Am J Ind Med 19:205-213